Decarbonizing hydrological landscapes through dam removal

ELSA BISBAL REGIDOR

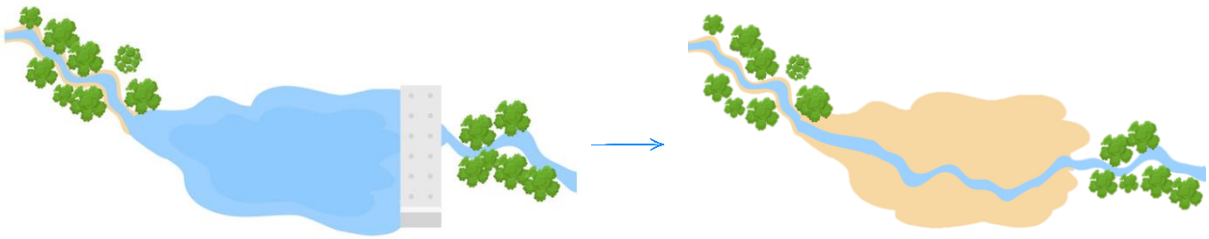

Màster d'Ecologia, Gestió i Restauració del Medi Natural, Universitat de Barcelona

Tutor: Daniel von Schiller (Universitat de Barcelona, Departament de Biologia Evolutiva, Ecologia i Ciències Ambientals)

Director: Rafael Marcé (ICRA/ CEAB-CSIC)

Centre d'Estudis Avançats de Blanes (CEAB-CSIC)

Barcelona, 10 de setembre del 2024

Decarbonizing hydrological landscapes through dam removal

ELSA BISBAL REGIDOR

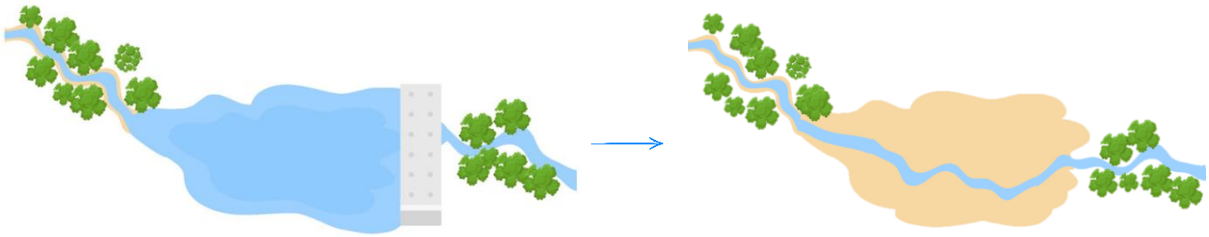

Màster d'Ecologia, Gestió i Restauració del Medi Natural, Universitat de Barcelona

Tutor: Daniel von Schiller (Universitat de Barcelona, Departament de Biologia Evolutiva, Ecologia i Ciències Ambientals)

Director: Rafael Marcé (ICRA/ CEAB-CSIC)

BISBAL REGIDOR ELSA - 47114122W

Firmado digitalmente por BISBAL REGIDOR ELSA - 47114122W
Fecha: 2024.09.09 11:36:37 +02'00'

VON SCHILLER CALLE, DANIEL GASPAR (FIRMA)

Firmado digitalmente por VON SCHILLER CALLE, DANIEL GASPAR (FIRMA)
Fecha: 2024.09.09 14:39:48 +02'00'
Versión de Adobe Acrobat: 2017.012.30262

Digitally signed by MARCE ROMERO RAFAEL - DNI ***4736** (46747362-T) on 09/09/2024 16:31 with a certificate emiited by AC Sector Público

Centre d'Estudis Avançats de Blanes (CEAB-CSIC)

Barcelona, 10 de setembre del 2024

ACKNOWLEDGMENTS

Throughout the entire process of this work, which began in May of last year, I have received support from many people. On one hand, the people at ICRA, who have become a solid support network and have made Girona feel like home. I am especially grateful to those who actively participated in the project: Lorena, with whom I shared almost every field campaign, turning them into something akin to summer camps; Carmen, for always being there and helping me with whatever I needed; Daniela and the two postdocs in the group, the two Danis (yes, in this group, everyone is named Dani except for me), for helping, guiding, and always being there. I also want to thank, of course, the project's PI, Rafa, for giving me the freedom I needed and always helping whenever necessary.

On the other hand, there are the people at the University of Barcelona (UB), my university, which after six years already feels like my second home. To Dani, Biel, Alba, and Lídia, for helping me with the calculations I couldn't do, for sharing protocols, and for letting me use their equipment. Among them, I especially want to thank Dani—without him, I wouldn’t be where I am now. Thank you for believing in me.

The third institution I would like to acknowledge is the UFZ in Germany, and Matthias, for always having their doors open for me, allowing me to process my samples there and saving me time and effort.

Finally, I want to thank all the people outside of science who have supported me during these chaotic two years of studying, working, and traveling: my family, lifelong friends, and the new friends I’ve made along the way.

In conclusion, I have been fortunate because, along the way, I have never been alone, and I can truly say that everyone I have crossed paths with has been wonderful and kind. I can only finish this work feeling grateful for everything I’ve learned and experienced. Thank you.

INDEX

ABSTRACT

Reservoirs are globally recognized as significant anthropogenic sources of greenhouse gases (GHG) to the atmosphere, particularly methane. However, the potential of dam decommissioning as a strategy to eliminate these emission hotspots in river networks has been largely overlooked. In this study, we assessed how dam removal reduces GHG emissions by comparing CO_2 and CH_4 emissions before, during, and after the demolition of a 5.6-meter tall dam in Spain. CO_2 and CH_4 flux measurements were conducted over one year in stream reaches upstream and downstream of the reservoir, within the reservoir itself, and in a control reservoir within the same catchment. Our findings reveal distinct variations throughout the dam removal process. Specially ebullitive CH_4, but also diffusive emissions were higher before decommissioning in the water, although the CO_2 released from sediments exposed to the atmosphere during and after decommissioning was considerably high. Additionally, we observed a pronounced seasonal effect on GHG emissions from the reservoirs, with total fluxes being higher in summer compared to winter at the two dam study sites. Overall, our results support the hypothesis that dam removal leads to a reduction in carbon emissions from the river network. In the context of global change, we anticipate that our findings will provide additional incentives for future dam removal projects, as they help to reduce anthropogenic GHG emissions.

RESUM

Els embassaments són reconeguts globalment com a fonts antropogèniques significatives de gasos d'efecte hivernacle (GEH) a l'atmosfera, especialment de metà. Tot i així, el potencial que té el desmantellament de preses com a estratègia per eliminar aquests punts crítics d'emissió en xarxes fluvials ha estat poc investigat. En aquest estudi, hem avaluat com la retirada de preses redueix les emissions de GEH comparant les emissions de CO_2 i CH_4 abans, durant i després de la demolició d'una presa de 5.6 metres d'altura a Espanya. Es van mesurar els fluxos de CO_2 i CH_4 durant un any en dos trams de riu aigües amunt i aigües avall de l'embassament, dins del mateix embassament i en un embassament de control dins de la mateixa conca. Els nostres resultats mostren variacions notables en les emissions durant tot el procés de retirada de la presa. Especialment les emissions ebullitives de CH_4, però també les emissions difusives, eren més altes en l'aigua abans del desmantellament, tot i que el CO_2 alliberat pels sediments exposats a l'atmosfera durant i després del desmantellament va ser considerablement alt. A més, vam observar un efecte estacional pronunciat en les emissions de GEH dels embassaments, amb fluxos totals més alts a l'estiu en comparació amb l'hivern en els dos llocs d'estudi de preses. En general, els nostres resultats donen suport a la hipòtesi que la retirada de preses condueix a una reducció de les emissions de carboni en la xarxa fluvial. En el context del canvi global, anticipem que els nostres resultats proporcionaran incentius addicionals per a futurs projectes de retirada de preses, ja que ajuden a reduir les emissions antropogèniques de GEH.

1. INTRODUCTION AND OBJECTIVES

Damming, land use changes, and other anthropogenic activities have profoundly altered fluvial ecosystems over the past decades and even centuries. Built to store water, generate hydroelectric power, control floods, and provide other beneficial services, hundreds of thousands of dams and small weirs, many of them no longer in use, fragment Europe's rivers (Schiermeier, 2018). Globally, estimations suggest that there exist 16.7 million reservoirs (Lehner et al., 2011). Although they can provide drinking water, irrigation and energy, this extensive dam construction has significantly altered inland water ecosystems, but also human societies (Kirchherr & Charles, 2016). Inland waters account for only 1% of the Earth's surface, yet they harbour 20% of its species (Fang et al., 2006). When considering vertebrates, about one-third of all species live in freshwater ecosystems, specifically freshwater fish, which account for about 40% of global fish diversity (Dudgeon et al., 2006). The frequent interruption of water flow through damming induces changes in streamflow regimes, sediment mobilization and wetland morphology and geomorphology (Donohue and Molinos, 2009, Wu et al., 2013), compromising its biodiversity (Vorosmarty et al., 2010).

While the impact of the lack of connectivity on biodiversity and ecosystem services has been extensively studied (Wu et al., 2019), the biogeochemical consequences of these alterations remain relatively unknown. Inland waters play a complex role in the global carbon cycle, not only by sequestering carbon but also by acting as significant sources of carbon emissions. River networks function as bioreactors, processing a significant portion of the organic carbon they transport. In fact, over half of the organic carbon entering these systems is either stored or emitted into the atmosphere following biological processing (Cole et al., 2007; Battin et al., 2009; Aufdenkampe et al., 2011; Raymond et al., 2013).

One might assume that inland waters, which account for only 0.3% of Earth's water compared to the 97.5% found in marine environments, would have a minimal impact on the global carbon budget. However, this assumption is far from accurate. Streams and rivers emit 1.8 ± 0.25 GtC yr^{-1}, while lakes and reservoirs emit 0.32 ± (0.26, 0.52) GtC yr^{-1} (Raymond et al., 2013), contributing to a global carbon flux that rivals the ocean's carbon sequestration capacity of approximately 2.5 ± 0.6 GtC yr^{-1} (Friedlingstein et al., 2020). Thus, inland waters play a disproportionate role in the global carbon budget, functioning both as carbon sinks and sources.

However, alterations to natural water flow can affect a river's capacity for carbon sequestration and emission by increasing the residence time of water, nutrients, and sediments. Carbon sequestration is the process of removing CO_2 and its derivatives from the environment and storing it in carbon pools for extended periods, out of reach of organisms capable of consuming

and degrading it, thereby preventing emissions (Lal, 2007; Farrelly et al., 2013). This process is particularly important in the context of global warming, as these carbon-sequestering systems capture a significant portion of the excess CO_2 released into the atmosphere (Lal, 2007). Hence, damming enhances carbon transformation, sedimentation, and retention (Maavara et al., 2020).

On one hand, dams can act as carbon sedimentation spots, removing carbon along with other nutrients from the water column through their sedimentation. On the other hand, this accumulation of carbon in the sediments can also be released through the emission of gases into the atmosphere (Downing et al., 2008). The decomposition of the organic matter stored in the reservoir produces carbon dioxide (CO_2) and methane (CH_4), two greenhouse gases (GHG) (IPCC, 2019). CO_2 is mainly the product of aerobic respiration, where O_2 is used as the electron acceptor, releasing CO_2 as a waste product. On the other hand, CH_4 is mostly produced in the anoxic bottoms of reservoirs as a byproduct of anaerobic respiration, where CO_2 is used as the final electron acceptor. CH_4 can be emitted to the atmosphere through three different pathways: ebullition (bubbling), diffusive emission and plant-mediated transport (Bastviken et al., 2004). However, among all these pathways, we will consider two: ebullition, which accounts for 65% of CH_4 fluxes from the surface waters of reservoirs, and diffusion, responsible for the remaining 35% when only considering these two emission pathways (Deemer et al., 2016).

CH_4 ebullition is quite unpredictable and difficult to quantify (Bastviken et al., 2008). It involves the formation of CH_4 bubbles in the sediments, which are released into the water preventing CH_4 from being oxidized in the water column, and consequently being directly emitted to the atmosphere from the water surface (DelSontro et al., 2016). This bubble release is controlled by multiple factors that decrease hydrostatic pressure, such as changes in water pressure (water level or atmospheric changes) (Engle & Melack, 2000; Eugster et al., 2011) or wind changes (Keller & Stallard, 1994), and increases in temperature, which reduce the solubility of CH_4 and increase its production in the sediments (Duc et al., 2010; Yamamoto et al., 1976). These bubbling emissions can account for more than 80% of all the CH_4 emitted in some inland stagnant water ecosystems (Bastviken et al., 2011).

In this way, reservoirs can contribute significantly to global carbon budgets, influencing global warming (Deemer et al., 2016). Specifically, it is estimated that reservoirs globally release approximately 0.8 Pg CO_2 equivalents every year, being responsible of ~1.5% of the global anthropogenic emissions (Deemer et al., 2016). The role of CO_2 emissions of anthropogenic origin is not very clear in the case of emissions from reservoirs. Lentic systems emit on average between 18 and 55 mmol $m^{-2}\,d^{-1}$ of CO_2 (Raymond et al. 2013, Deemer et al. 2016), while lotic

systems emit between 120 and 633 mmol m^{-2} d^{-1} (Raymond et al. 2013, Borges et al. 2015). In this way, the anthropogenic impact of the construction of reservoirs is ambiguous. Worldwide, CH_4 emissions are estimated to be responsible for approximately 20% of current global warming (Kirschke et al., 2013). CH_4 emissions have a clear anthropogenic origin, with reservoirs globally emitting 10.1 Tg of CH_4 annually (Johnson et al., 2021). CH_4 is a greenhouse gas that is 27.9 times more potent than CO_2 over a 100-year period (GWP, AR4, IPCC). These high emissions and their strong capacity to act as a GHG are especially relevant in reservoirs, as 79% of their CO_2-equivalent emissions are in the form of CH_4 (Deemer et al., 2016).

The high GHG emissions, especially of CH_4, make us question whether the hydropower generated in reservoirs is as green as we previously thought. In fact, in certain reservoirs, the emissions corrected for power density can be even higher than those from energy production through coal burning (Gómez-Gener et al., 2023).

Considering the aforementioned emissions, dismantling dams is increasingly suggested as a method to mitigate anthropogenic emissions, a proposal that aims to address various ongoing issues. On one hand, the demolition of dams that are about to expire or are in poor condition is economically more feasible than restoring and maintaining them for another 50 or 100 years (Doyle et al., 2003). In this way, the river environment is restored, future investment is reduced, and public health for the local population is improved (Perera et al., 2021). On the other hand, dam removal has potential as an alternative to decrease anthropogenic emissions from river networks. This approach, however, has a clear drawback: global carbon emissions appear to be lower than the organic carbon burial stored in reservoir sediments (Deemer et al., 2016; Mendonça et al., 2017). Consequently, during the dam removal this huge amount of carbon stored in the sediment can be decomposed and released emitting even more CO_2 and CH_4 (Perera et al., 2021). Once the dam has been dismantled, the problem is still present. The sediment remains permanently exposed until ecological succession occurs, releasing CO_2 to the atmosphere.

Exposed sediments are hotspots for CO_2 emissions. They release even more CO_2 than lotic systems, emitting between 4 and 1533 mmol m^{-2} d^{-1} (Gómez-Gener et al., 2016; Obrador et al., 2018), due to the higher availability of oxygen in the air, which accelerates the aerobic respiration of accumulated organic matter (Keller et al., 2020). On the contrary, the sediments practically do not emit any methane (0.1–1 mmol m^{-2} d^{-1} ; Yang et al., 2014; Gómez-Gener et al., 2015), since it oxidizes when it comes into contact with the air, and therefore, with O_2. Thus, CH_4 emissions from dry sediments are much lower than those emitted by aquatic systems (lotic and lentic; Stanley et al., 2016; Deemer et al., 2016).

This difference raises a question. While there are already many studies showing that GHG emissions are higher in reservoirs than in adjacent lotic systems (Deemer et al., 2016), little is known about what happens to these fluxes when dams are dismantled. Is the reduction in CH_4 emissions sufficient to compensate for the subsequent increase in CO_2 emissions from exposed sediments? It could happen that during the drawdown of the dam, total fluxes increase due to higher fluxes from exposed sediments. In a study conducted in Navarra, emissions from exposed sediments accounted for an average of 93% of the CO_2 flux and 87% of the flux expressed in CO_2-eq. However, emissions from this study site were dominated by CO_2 fluxes (contributing 99% of total C fluxes) (Amani et al., 2022). These results could be different in a reservoir that previously emitted higher quantities of CH_4 than CO_2. Therefore, even if CO_2 emissions increase after removal, total emissions, particularly CH_4, would have been higher before decommissioning.

To truly evaluate the success of dam removal in mitigating anthropogenic GHG emissions, it is necessary to comprehensively study the fluxes from both the water and the exposed sediments. Only in this way can we determine if dam decommissioning is an effective strategy for removing CH_4 emission hotspots from river networks, thus decarbonizing the landscape and reducing emissions. In this study, we want to asses if dam removal decreases anthropogenic greenhouse gas (GHG) emissions, particularly CH_4. We hypothesize that anthropogenic GHG emissions from a dammed stretch of a Mediterranean river network decrease when a dam is dismantled, and flow continuity is restored. To achieve that, we define the following specific objectives:

1. To evaluate the annual variability of GHG emissions from both free-flowing river reaches up and downstream the dam, and from the dammed reaches. We hypothesize that GHG emissions are lower in the free-flowing river reaches compared to dammed reaches.
2. To evaluate the impact of dam removal on GHG emissions from dammed reaches. We hypothesize that dam removal will severely decrease GHG emissions from the former dammed reaches, particularly CH_4, resulting in a transition towards the dynamics observed at the free-flowing reaches.
3. To explore the suitability of dam removal as a strategy for reducing anthropogenic GHG emissions from river networks. we hypothesize that dam removal can be an effective method for reducing anthropogenic GHG emissions, particularly in reservoirs with significant CH_4 emissions.

2. METHODS

2.1. STUDY SITE

The study site is the weir of the Former Colonia Rio, with a height of 5.6 m and a width of 50m, located adjacent to the village of Monistrol de Calders in Catalonia, in the northeast of the Iberian Peninsula (Figure 1). Constructed more than a century ago, it had a maximum depth of 3 m. The stream is situated in the upper part of the Llobregat basin, near the natural park of Sant Llorenç de Munt i l'Obac. This particular weir was selected for this study because it was the only dam dismantled by the Catalan Water Agency (ACA) during 2023-2024. The dam was dismantled to restore the river's connectivity. Additionally, our participation in the study of the dam was also included in the demolition plan. It was anticipated that the biogeochemical study may provide further arguments for ACA in favour of dismantling such structures.

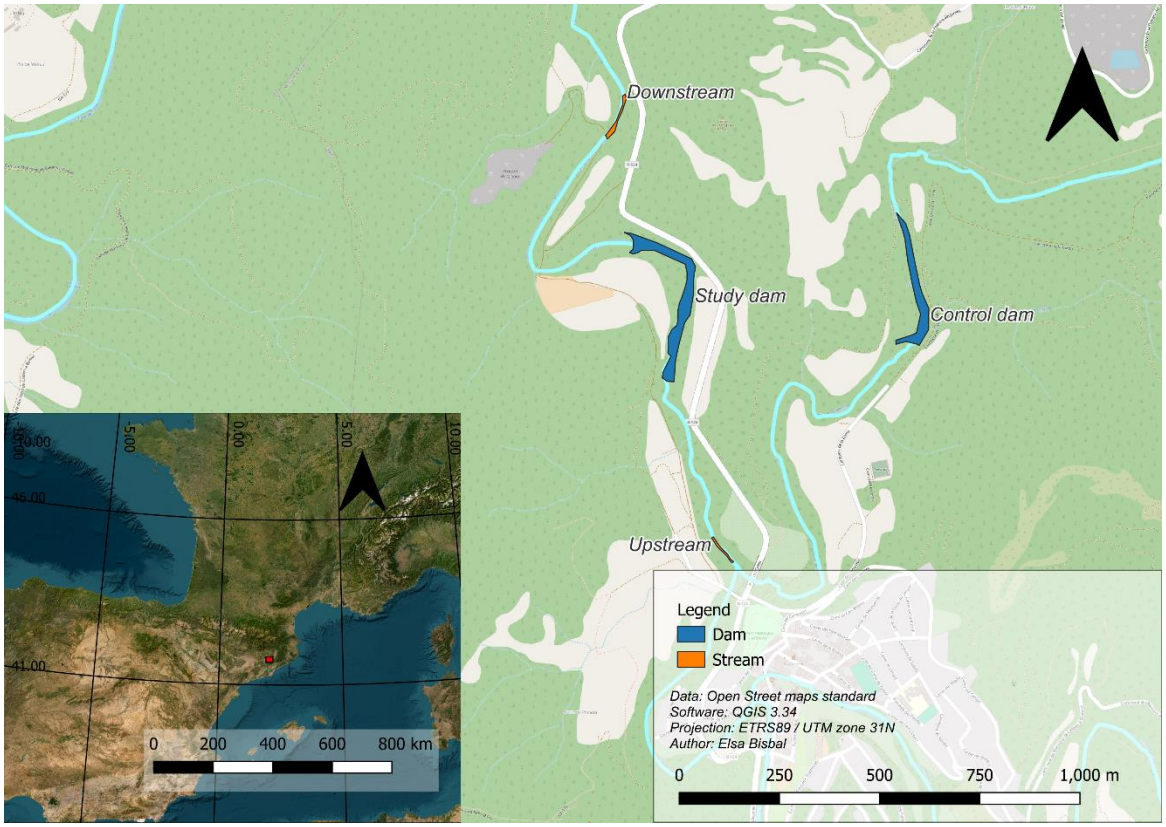

Figure 1: On the left-bottom, the location of the study dam on the Iberian Peninsula (41°46'11"N 2°00'33"E). On the right, an enlarged map of the area with the different study points: the study dam, the control dam and upstream and downstream sites (QGIS 3.34).

The dam is surrounded by riparian forest in the upper reaches and tall reeds at the dam. Additionally, agricultural fields and a pig farm are located adjacent to the dam. These factors can contribute to the eutrophication of its waters. The region experiences a Mediterranean

climate, with dry, hot summers and moderately cold winters with occasional frost. Moreover, part of the sampling period coincided with a prolonged drought in the area.

2.2. SAMPLING DESIGN

We selected three types of sampling sites: the dam to be removed, riverine sites, and a control dam. The removed dam was sampled before, during, and after the decommissioning. The sampling was constrained by the date of the demolition, as it had to be structured with 2 clear periods: before and after the decommission. The pre-demolition period was short, as we started the samplings on May 2023 and the dam was demolished in October 2023.

To account for the annual variability of the GHG emissions from the dam, we selected a similar dam within the same basin, located a few kilometres upstream of the study dam, as a control. We also took samples from riverine sites downstream and upstream from the dam. These river reaches are expected to resemble the dam site once it has been demolished.

Sampling was conducted from May 15, 2023 to February 12, 2024, once or twice per month. In total, 11 samplings were carried out during this period.

Figure 2: Number of sampling campaigns conducted per month. In orange, the samplings before the demolition; in green, after the demolition.

2.3. CARBON EMISSION MEASUREMENTS

2.3.1. Carbon emissions in lentic conditions

In this section, we consider the three types of study sites, including the river reaches when they were stagnant or not flowing. Thus, we have three possible cases: the study dam before being demolished, the control dam throughout the study, and the river reaches during dry periods when the water was not flowing.

Emissions of both CO_2 and CH_4 were measured using floating chambers. These were anchored and left to incubate. The incubations had three durations: short, lasting between 3 and 5 minutes; medium, lasting between 3 and 7 hours, that were left during the day; and long-term ones, lasting more than 8 hours, which were left overnight.

For measuring CO_2 fluxes, we used short-duration incubations. We conducted them with an IRGA (Infrared Gas Analyzer, EGM-4 from PPSystems) connected through a closed loop with the floating chamber. This device provides CO_2 values in ppmv over time.

For CH_4, we used all three types of incubations. In three campaigns during July and August, we had the support of a PICARRO Gas Scouter (gas concentration analyser), which allowed us to measure both CO_2 and CH_4 continuously during the short incubations. For the remaining incubations and campaigns, we directly collected air samples from inside the chamber at the beginning and end of each incubation. We stored those samples in pre-evacuated Exetainer vials. The Exetainers (Labco, UK) are 12 mL capacity vials specially designed for gas sampling. We injected nearly 60 mL of air into each vial, generating an overpressure to reduce the risk of contamination from external air.

Moreover, we took samples to obtain the concentrations of CO_2 and CH_4 from the water at each of the sampling points. To do this, we used a 60 mL syringe to apply the head-space method. We filled the first 30 mL with water, and the remaining 30 mL with a gas of known concentrations (either atmospheric air or nitrogen). With this mixture, we agitated the syringe and let the concentrations equilibrate at a controlled temperature, in this case, the temperature of the surface water. Finally, after a few minutes, the concentration in the water will have equilibrated with that of the air, and then we can inject the sample into a pre-evacuated Exetainer.

The content of the Exetainers were subsequently analysed with a gas chromatograph equipped with a flame ionization detector (FID) either at the University of Barcelona (UB, GC 7820A, Agilent, Santa Clara, CA, USA) or at the Helmholtz Centre for Environmental Research (UFZ) in Magdeburg, Germany (GC 6810C, SRI Instruments, USA). For this analysis, a known volume of the sample was injected into the chromatograph, where it passed through a column that separated the elements from each other (CO_2 and CH_4). At the end of the column, there was a flame where they underwent combustion. As a result, a combustion peak was obtained for each element, with an area that was easily calculable. Using a calibration curve, this area value was then converted into gas concentrations.

2.3.2. Carbon emissions in lotic conditions

We consider lotic systems as any of the study sites where water flows. This includes river sections if flowing, and the study area of the dam once it was dismantled and water was flowing. In this type of conditions, we took headspace samples from each sampling point. With this, we obtained the concentrations of CO_2 and CH_4 in the water.

To calculate gas fluxes from these concentrations, we need the reaeration rate, which can be determined by performing a trace gas addition experiment. The additions were done with propane and salt because neither of these elements are consumed by fluvial metabolic pathways. Thus, any detected loss of the gas would have been emitted into the atmosphere, allowing us to calculate the reaeration rate. We made the addition following the Jin *et al.* 2012 protocol, in transects of 60 to 120 meters, depending on water speed and flow. We used conductivity-meters to detect the arrival of the propane peak with the salt at 3 (upstream and downstream river sites) or 4 (removed dam) points along the transect, and when it arrived, we took 3 headspace water samples at each point. These headspace samples were injected into Exetainers and analysed afterward using gas chromatography at the CCiTUB (Shimadzu GC-2025).

Additionally, we measured the average width and depth of each study section. With this information and the data generated from the addition, we determined water velocity and flow rate values.

Finally, we placed a level sensor (Levelogger and Barologger Solinst, model 3100 M1.5) upstream and downstream of the dam to measure changes in water level and temperature every 15 minutes from September 28, 2023 until the end of the sampling period.

2.3.3. Carbon emissions from exposed dry sediments

The study dam dried up towards the end of summer, exposing sediment that had accumulated over time. This sediment was sampled for the first time on the campaign of September 13, 2023. Subsequently, demolition of the dam began, and it was emptied, exposing much of its sediment to the atmosphere. This sediment was sampled using soil chambers, which are driven into the ground and left to incubate for a known period. The river sections also dried up considerably in summer, but still did not leave exposed sediment for measurement because the riverbed is mostly bedrock. Finally, although the water level of the control dam also decreased considerably, it was not enough to expose its sediments.

For CO_2 sampling, the chambers were connected to an IRGA through a closed loop, and the incubation lasted for 5 minutes. For CH_4 sampling, an initial air sample was taken just when the chamber was driven into the ground, and a final sample was taken at the end of the incubation (medium or long-term incubation duration, 2.3.1.). The air samples were collected with a syringe and stored in Exetainers.

2.4. CO_2 AND CH_4 FLUX CALCULATIONS

2.4.1. Lentic conditions

2.4.1.1. CO_2 diffusive fluxes

For calculating diffusive emissions, we used floating chambers. This method was employed in the study dam during the pre-demolition period and afterward at the points furthest from the dam's mouth, where the water remained stagnant until strong floods carried away the sediment. Additionally, we used floating chambers in the control dam throughout the entire sampling period and in the river reaches during late summer. We calculated fluxes from the data generated by the IRGA or PICARRO.

We obtained a linear change in CO_2 concentration over time, expressed in fractional abundance (ppmv). By multiplying the slope of this change by the atmospheric pressure, we derived the CO_2 flux in pressure units (atm) over time. To standardize the flux (mmol m^{-2} d^{-1}), we converted this value using the ideal gas law (Equation, that was adapted to our data using Equation 2.).

$$PV = nRT \quad \{1\}$$

$$\frac{PCO2 \cdot Patm \cdot Vchamber}{R \cdot T \cdot s} = \frac{n}{s} \quad \{2\}$$

where the volume and surface area correspond to those of the floating chamber, the temperature is the average atmospheric temperature during the incubation, R is the ideal gas constant (0.082057 L atm K^{-1} mol^{-1}), and the pressure is the flux pressure value. The ideal gas equation was used to convert from pressure units to mass, and then everything was divided by the surface area of the chamber to obtain an emission per unit of surface area.

We obtained a flux rate for each incubation, having replicates per site and day. To standardize the values, we calculated an average per site and day.

2.4.1.2. CH_4 diffusive fluxes

CH_4 fluxes are more complex to calculate, as they combine two types of flux: diffusive and bubbling. In an incubation, it is difficult to differentiate which corresponds to which. Therefore, to calculate the diffusive fluxes, we disregarded the incubations and followed Fick's Law (formula 3). For this, we used the CH_4 and CO_2 concentrations obtained by headspace in the field. These will be the water concentrations for each sampling point. The atmospheric fractional abundance is assumed to be 1.8 ppmv for CH_4 and 421.2 ppmv for CO_2 (Global atmospheric concentrations (2020, NOAA)).

$$Flux = K_{gas} \cdot (C_{water} - C_{air}) \quad \{3\}$$

To obtain the diffusive flux, we first needed to calculate the K value, which corresponds to the reaeration rate for a specific gas (in this case, CH_4). This K value refers to the rate at which a gas is transferred from the water to the atmosphere, and is strongly related with the turbulence at the water's surface. For this calculation, we used the CO_2 flux values obtained in the previous section. Given the CO_2 concentrations in both water and air, along with the final flux value, the only unknown was the K (CO_2) value. We isolated and calculated it. Next, we converted it to K_{600} by applying the Schmidt equation (4) and then calculated the final K(CH_4) using the same equation.

$$K_{600} = \left(\frac{600}{Sc_{gas}}\right)^{-0.5} \cdot K_{gas} \quad \{4\}$$

Each gas has a specific known Schmidt number (Sc_{gas}), which depends on the water temperature during headspace equilibration. It allows us to convert the K_{600} of any gas (K_{gas}) to a standardized and generic K_{600} (Raymond et al., 2012).

The diffusive CH_4 flux will be the difference between the CH_4 in the water and the CH_4 in the air multiplied by the calculated K for CH_4. Thus, we obtain a CH_4 flux value for each incubation. As before, we make an average per each sub-sampling point. Hence, we obtain a flux value per sampling site and date.

2.4.1.3. CH_4 bubbling fluxes

The bubbling fluxes were calculated using incubation chambers. For this, the 3 types of incubations were used: short, medium, and long duration. Thus, a regression was performed between the increase in CH_4 and the incubation time, resulting in an initial flux in ppmv s^{-1}.

The issue is that this flux needs correction. On one hand, if bubbling is very low but there is significant diffusion, not accounting for it will overestimate the flux by attributing diffusion to bubbling, which is incorrect. On the other hand, if the bubbling flux is actually high, resulting in a higher concentration of CH_4 in the chamber than in the water, a back-diffusion process occurs where methane is reabsorbed into the water. Therefore, solely relying on the difference in CH_4 in the chamber over time can easily lead to overestimating or underestimating the bubbling flux.

To address this issue, we calculated the bubbling flux by estimating a continuous CH_4 diffusive flux throughout the entire incubation, using the CH_4 concentration of the water and the K (CH_4) value (2.4.1.2.). This diffusive flux varied according to the CH_4 concentration in the chamber.

With this rate, we corrected the bubbling flux and estimated the flux required to reach the final CH_4 concentration, considering the diffusive flux.

So, we obtained a bubbling value (mmol CH_4 m^{-2} d^{-1}) for each of the incubations conducted, whether short, medium, or long duration.

2.4.2. Lotic conditions

As mentioned in 3.3.2., we used this calculation for the river sites when the water flowed and for the demolished dam. As we did not use floating chambers, both CO_2 and CH_4 diffusive fluxes were calculated the same way.

To calculate the flux rate, we used Fick's Law {3}. The water concentration value was obtained from the headspace samples, both for CO_2 and CH_4. The atmospheric fractional abundance was assumed to be 1.8 for CH_4 and 421.2 ppmv for CO_2 (Global atmospheric concentrations (2020, NOAA)).

To calculate the reaeration rate (K), we used the data from the propane addition. For this, we corrected the area obtained from the propane peak at each sample collection point by the difference between the peak conductivity and the baseline (pre-addition) conductivity. This corrects for the amount of propane that was not emitted into the atmosphere but rather dispersed and diluted along the river. To determine the general K600, we first calculated $K_{propane}$ by performing a regression between the logarithm of the corrected conductivity and the arrival time. The slope of this regression was multiplied by the average depth of each section (measured manually) to obtain $K_{propane}$ (Jin et al., 2012). To calculate the standardized K_{600}, and thus be able to convert it for CO_2 and CH_4, we used the conversion through the Schmidt number (equation 4).

Thus, we multiplied the concentration differential (C_{water} - C_{air}) by the K for each gas and obtained the CO_2 and CH_4 flux (mmol m^{-2} d^{-1}) for each sampling sub-point. Finally, we averaged these fluxes for each sample collection point and then calculated a second weighted average based on the area they occupied, calculated with the widths measured manually. In this way, we obtained a flux value and its accumulated error for each sampling day and each study site (upstream, downstream, and the study dam).

Finally, it is worth noting that bubbling fluxes in rivers and areas where water flows were not considered. Therefore, rivers only had diffusive fluxes, including during dry periods when water was stagnant and flux measurements were conducted using floating chambers.

2.4.3. Dry sediments

This calculation was only used for the exposed sediments in the study dam. For this, we used soil chambers. The procedure was the same as with the floating chambers (2.4.1.1.). We obtained CO_2 values over time in fractional abundance units (ppmv s^{-1}) and then convert it to pressure and mass units using the ideal gas equation {1}. This new flux value (mmol s^{-1}) was divided by the surface area of the chamber to get the flux per unit area, and finally, the seconds were converted to days. Thus, we obtained a flux (mmol m^{-2} d^{-1} for each incubation. As in the other cases, an average was taken for each sampling sub-point obtaining a unique value of CO_2 flux per sampling site and day with its error.

2.5. TEMPORAL INTEGRATION OF CO_2 AND CH_4 FLUXES

2.5.1. Upstream and downstream

The river sections had two types of fluxes: diffusive CO_2 and diffusive CH_4. In these sections, we aimed to have continuous gas flux data for the entire sampling period (from May 2023 to February 2024). To achieve this, we used flow data calculated from the additions and the installed level sensors. This helped us estimate continuous K_{600} values throughout the period.

2.5.1.1. K_{600} estimation

To calculate the daily K_{600}, we related it to the river flow. To do this, we first needed to estimate the daily flow rate. On one hand, we had the level sensors. However, these were installed on September 28, 2023, so we lacked flow data from May 15, 2023, to September 27, 2023. To address this, we used data from a nearby stream gauging station within the same watershed (Riera Gavarresa, Artés). We related its flow data to those obtained in our sampling. We used the flow measured in the field from the upstream section for comparisons, as it was less affected by drought periods being located above the dam, where water continued to flow almost throughout the summer. Therefore, we had more flow data from this section. We performed a semilogarithmic regression between the flow rate upstream and the flow rate of this stream, obtaining a continuous flow rate for upstream.

From 28/09/2023 onwards, we used the data from the water level sensor installed upstream of the dam, which allowed us to calculate the water level continuously. After averaging this value daily, we performed a second power regression between the flow rate of the upstream section and the water level of this section. With both regressions, we obtained the continuous upstream flow rate throughout the entire campaign.

To complete the flow rate analysis, we conducted a third potential regression that allowed us to calculate the downstream flow based on the upstream flow.

On the other hand, we had the estimation of K_{600} based on flow rate. We conducted a linear regression between the calculated flow rate in each of the additions and the corresponding K_{600} obtained from them, separately for upstream and downstream.

Finally, we used this newly found relationship to calculate the daily continuous K_{600} for the entire sampling period based on the estimated flow rate. The formula differs for each river section.

To summarize, we used the following formula to calculate the effective K_{600} for each section and date:

$$K_{600}(upstream, 15/05\text{- }27/09) = \left(6.91 \cdot \ln\left(Q_{gav}\right) + 42.561\right) \cdot 0.372 \quad \{5\}$$

$$K_{600}(upstream, \text{from } 28/09/23\text{-on}) = (10^9 \cdot (Level)^{13.58}) \cdot 0.372 \quad \{6\}$$

$$K_{600}(downstream, 15/05\text{-}27/09) = 0.26 \cdot (6.91 \cdot \ln\left(Q_{gav}\right) + 42.561)^{1.31} + 0.032 \quad \{7\}$$

$$K_{600}(\text{downstream, from } 28/09/23\text{-on}) = 0.29 \cdot (0.26 \cdot (10^9 \cdot \ln(Level)^{13.58})^{1.31}) + 0.032 \quad \{8\}$$

Where Q_{gav} is the waterflow value from the Riera de les Gavarres station during the period from 15/05 to 27/09, and Level represents the water level in the upstream section of the river.

2.5.1.2. Concentration values

The CO_2 and CH_4 concentration values could not be correlated with any of the available variables. Therefore, the values obtained for each period were directly interpolated to obtain continuous data.

2.5.1.3. Final flux calculation

Finally, we applied the Schmidt equation to correct the K_{600} for each gas, and then applied Fick's Law again to obtain the fluxes. In this way, we obtained continuous flux values for the entire sampling period.

To compare the CO_2 fluxes with those of CH_4, considering that CH_4 is a much more potent greenhouse gas than CO_2, we multiplied the CH_4 flux by 27.9 to obtain the CO_2 equivalents for this gas (100-year GWP (AR6), IPCC 2021). Finally, we conducted an ANOVA test to evaluate the differences between upstream and downstream sites (RStudio, 2023.03.1+446).

2.5.2. Removed dam

The dam emits both CO_2 and CH_4 diffusively, along with CH_4 by bubbling. These three fluxes occur simultaneously while the water is stagnant in the reservoir. We had a value for each of these fluxes for each sampling day. While the dam was standing, we calculated the three fluxes using the floating chambers. Once it was removed, the first two sampling points (those near the mouth of the dam) had no bubbling emissions, and we calculated their diffusive fluxes using Fick's Law. Finally, we had a third type of flux: that emitted by the sediments exposed after the dam's demolition. These fluxes, initially non-existent, started to occupy a significant portion of the sampling area, primarily at points closest to the dam's mouth.

The total fluxes emitted by the dam included those released by the water while it was intact, as well as those from the water and exposed sediments after the dam was demolished. Therefore, we calculated the proportional area occupied by water and sediment at each sampling point after the demolition. Using this area, we created a weighted average of the water and sediment fluxes based on the surface area each one occupies, resulting in a single combined flux. By applying this weighted average to all sampling points, we obtained a final total flux for the entire dam for each sampling day.

To conclude and to compare which type of flux contributes most to the emissions, we converted the CH_4 fluxes (diffusive and bubbling) into CO_2 equivalents by multiplying their value by 27.9 (100-year GWP (AR6), IPCC 2021).

2.5.3. Control dam

The control dam only had emissions originating from the water, as it did not expose sediments at any point during the sampling period. Therefore, its final integration consisted of calculating a weighted average for the area occupied by each of its three sampling points for each type of flux (diffusive CO_2, diffusive CH_4, and bubbling CH_4). This provided a single flux value (mmol m^{-2} d^{-1}) with its associated calculation error for each sampling day. Finally, as in the other study sites, the CH_4 fluxes were converted to CO_2 equivalents by multiplying them by 27.9 (100-year GWP (AR6), IPCC 2021).

2.5.4. Uncertainty propagation

Throughout all the previous calculations, we accumulated a considerable number of variables, each carrying its own associated error: from average values and transformations to the K_{600} calculations (5:8 equations), and beyond. Even the total flux sum had uncertainty associated.

To accurately estimate the total error in our final calculations and assess the reliability of our flux values, we employed a Monte Carlo approach. Monte Carlo is a powerful statistical method used to model uncertainty and variability in complex systems. It involves generating a large number of random samples (10.000 in our case) from input distributions based on our calculated averages and associated errors. In our case, we used the software R-studio (2023.03.1+446 version, library propagate; Spiess 2018).

For both dammed sites—the target reservoir and the control site—we applied the model after calculating the fluxes for each emission pathway: CO_2, CH_4 diffusive, and CH_4 bubbling. To do this, we calculated the error associated with each average daily flux calculation, which, in this case, depended solely on the error linked to averaging our replicates (both in water concentrations and total fluxes). We then constructed a distribution for each of the three emission pathways, using the obtained mean and its associated error. Thus, we obtained as many distributions as there were emission pathways: three for the control site (the three mentioned above) and five for the target reservoir (adding the CO_2 and CH_4 diffusive emissions from the sediment).

Once we created the distributions, we input an equation into the model that summed these fluxes, and in the case of the target reservoir, we weighted the fluxes by the area occupied by water and the area occupied by exposed sediment for each sampling day. We ran the model, performing 10.000 iterations. This process produced a new distribution of all possible results from the previous combination. From this new distribution, we took the mean, which represented the final total flux, and the standard deviation of the distribution, which indicated the accumulated error throughout the entire process.

For the river, however, the process was a bit more complex. The fluxes were calculated continuously along with the estimation of their parameters. Thus, for each emission pathway (in this case, only diffusive CO_2 and CH_4), the following variables were considered: the concentrations in the water and their associated error (calculated by averaging the headspace samples obtained and their error), and the K_{600} (with the error associated with its calculation). Since the estimation of K_{600} carries a significant amount of error by itself, we first performed an initial Monte Carlo simulation that included this calculation, obtaining the continuous total flux for each of the two emission pathways (CO_2 and CH_4).

Therefore, the equation inserted into the model was the concentration in the water (with error) minus that in the air (as a fixed variable, it had no associated error), multiplied by the equation necessary for calculating K_{600} (equations 5:8), according to Fick's Law {3}. After this, we performed a final Monte Carlo simulation by summing the two emission pathways (diffusive CO_2 and CH_4) to obtain the final distribution for each river section, upstream and downstream.

Thus, the following results represent the mean value of this output distribution and its standard deviation, obtained from the Monte Carlo model.

3. RESULTS

3.1. RIVER EMISSIONS

The total emissions from the two river sections fluctuated around 260 mmol m^{-2} d^{-1} (11,44 gCO_2-eq m^{-2} d^{-1}, upstream) and 192 mmol m^{-2} d^{-1} (8,45 gCO_2-eq m^{-2} d^{-1}, downstream). No significant differences were observed between these two river sections (ANOVA, p-value = 0.1068), although significant differences were observed in the interaction between the sections and the date (ANOVA, p-value = 0.0016). Although the average remained relatively consistent throughout the entire analysed period, some emission peaks were observed, especially towards the end of this period, along with greater oscillations.

Moreover, the significant differences in the interaction between the date and the mean emissions disappeared in mid-November, with the removal of the dam (ANOVA, p-value > 0.05).

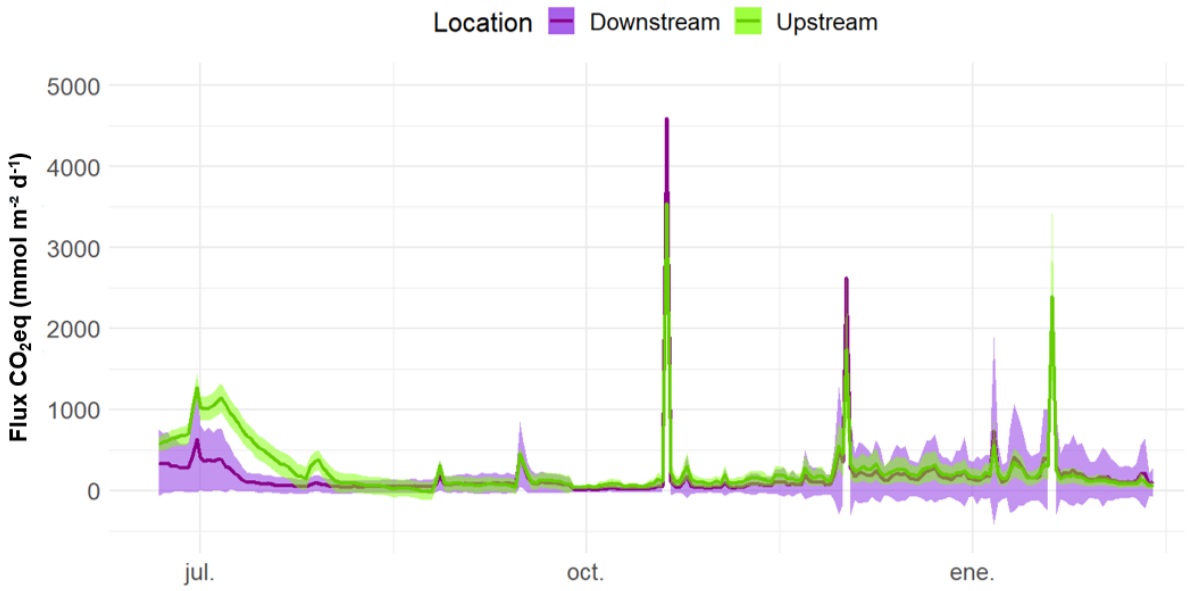

Figure 3: total fluxes (CO_2 and CH_4) expressed in CO_2 equivalents for both upstream (green) and downstream (purple) riverine sites with the standard deviation estimated with a Monte Carlo approach, from June 2023 to February 2024.

3.2. REMOVED DAM EMISSIONS

Figure 4 illustrates the total emissions from the reservoir, expressed in CO_2 equivalents (CO_2, diffusive CH_4, and ebullitive CH_4) from both the water and the exposed sediment. Initially, total fluxes were quite high until October, ranging between 500 and 2000 mmol CO_2-eq m^{-2} d^{-1}, and then decreased to between 0 and 500 mmol CO_2-eq m^{-2} d^{-1}. This shift coincided with the timing of the dam's demolition. Therefore, total GHG emissions decreased following the dam's dismantling.

The contribution of each emission pathway to the total flux also changed over time. Firstly, exposed sediments emissions began to appear in September and became increasingly significant over time. Additionally, bubbling was the dominant emission pathway in all campaigns conducted prior to the demolition. Thus, when the dam was intact, the CH_4 bubbling pathway was the most significant emitter compared to the other pathways. However, this was not happening any more after the demolition. In February, bubbling was not even detectable.

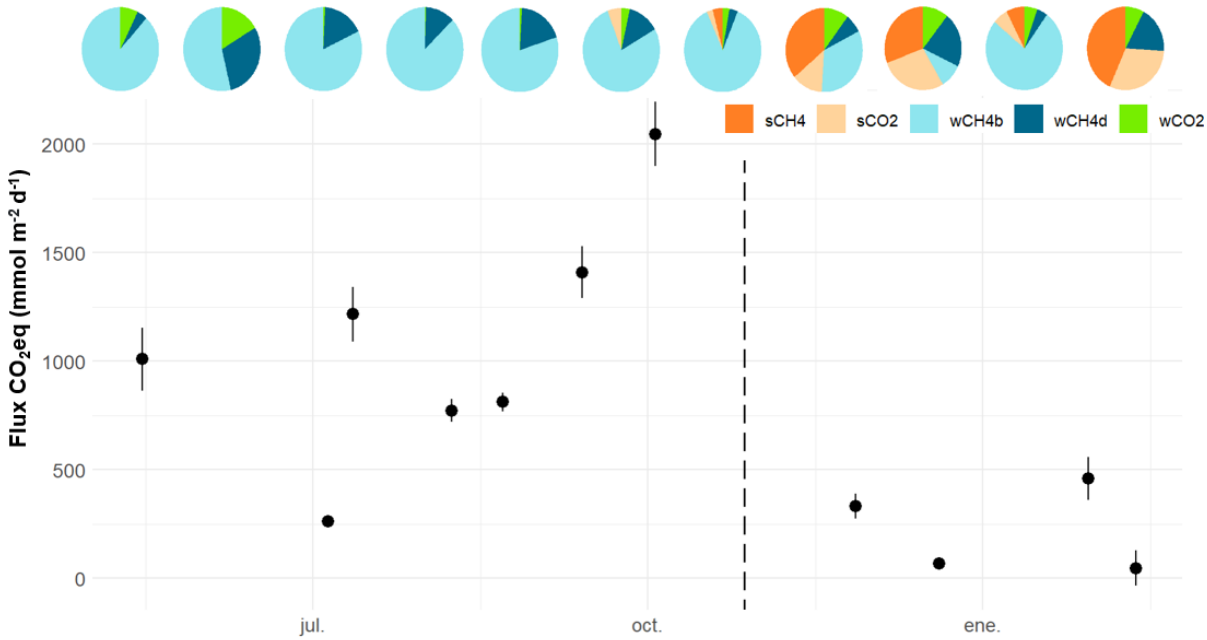

Figure 4: Total fluxes (CO_2, diffusive and ebullitive CH_4) expressed in CO_2eq from both water and sediments along the 11 sampling campaigns. Pie charts at the top of the graph show the percentage contribution of each emission pathway to the total flux: CH_4 emitted from dry sediment (sCH_4, orange), CO_2 emitted from dry sediment (sCO_2, light orange), ebullitive CH_4 from the water (wCH_4e, light blue), diffusive CH_4 from the water (wCH_4d, dark blue), and CO_2 emitted from the water (wCO_2, green).

Additionally, we grouped the total fluxes into two categories: before and after the demolition (Figure 5). The mean total flux before the removal was 1075.06 mmol CO_2-eq m^{-2} d^{-1} (47.34g CO_2-eq m^{-2} d^{-1}), while the mean total flux after the removal was 227.34 mmol CO_2-eq m^{-2} d^{-1} (10.0g CO_2-eq m^{-2} d^{-1}). There were significant differences between the two conditions (ANOVA test, p-value of 0.0191).

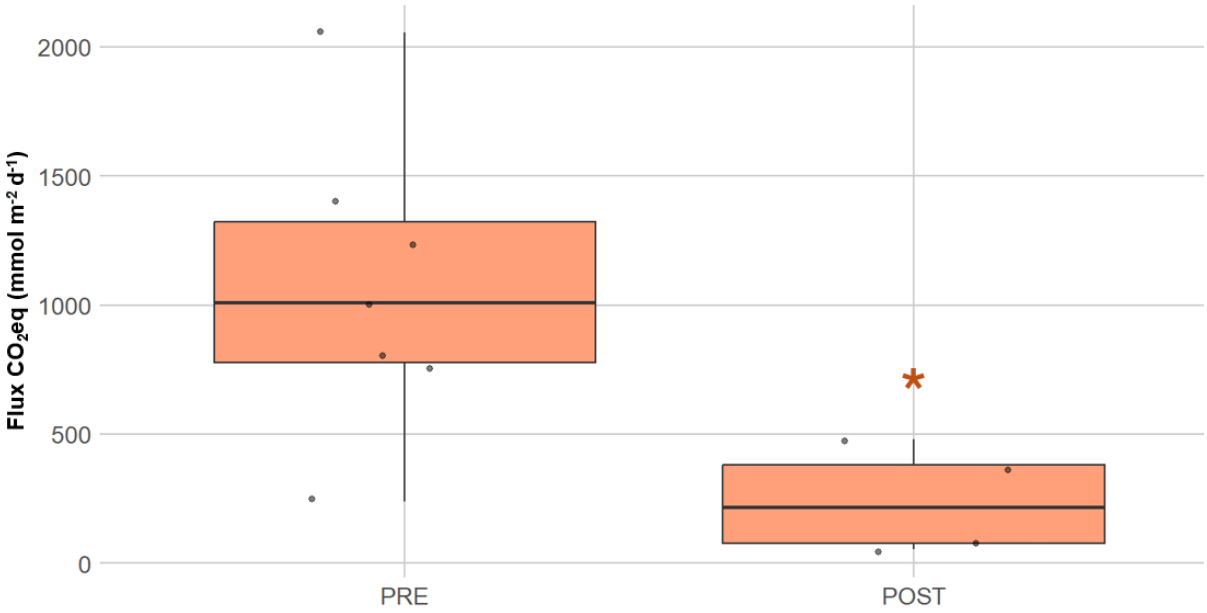

Figure 5: Boxplot of the total fluxes (CO_2, diffusive and ebullitive CH_4) expressed in CO_2eq before and after the dam demolition.

3.3. CONTROL DAM EMISSIONS

The total emissions from the control reservoir (CO_2, diffusive CH_4, and ebullitive CH_4) were much lower than those from the study dam. The maximum emission was 383.95 mmol CO_2-eq m^{-2} d^{-1}, while the minimum was 0 mmol CO_2-eq m^{-2} d^{-1}. The minimum value corresponded to the December campaign, when the reservoir was completely frozen. A decreasing trend in total emissions was observed throughout the study period. There were significant differences between summer-autumn (until October) and autumn-winter (November-Feburary) periods (ANOVA test, p-value = 0.0051), During the warm period, with temperatures over 20ºC, the mean total flux was 253.4 mmol m^{-2} d^{-1} (11.15gCO_2-eq m^{-2} d^{-1}). In contrast, during the cold period (temperature reaching below 0 values) the mean total flux was 64.38 mmol CO_2-eq m^{-2} d^{-1} (2.83 gCO_2-eq m^{-2} d^{-1}).

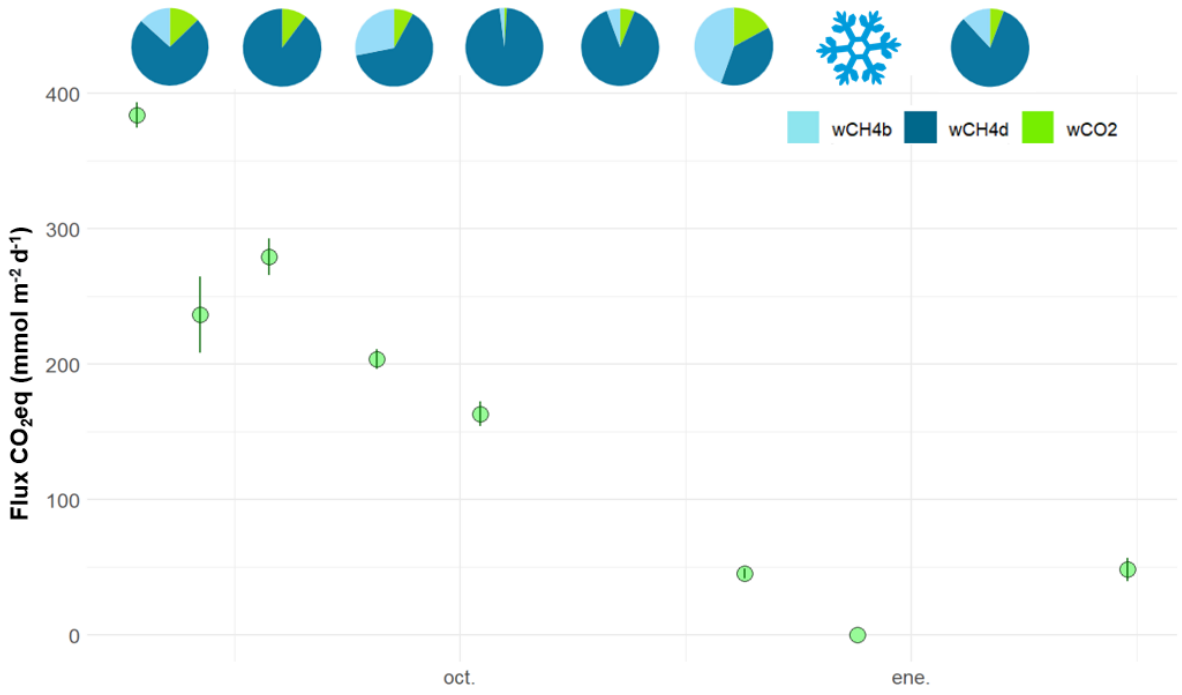

Figure 6: Total fluxes (CO_2, diffusive CH_4, and ebullitive CH_4) expressed in CO_2 equivalents with the associated standard deviation (Monte Carlo approach). At the top, pie charts show the percentage contribution of each emission pathway: CH_4 bubbling (light blue), diffusive CH_4 (dark blue), and CO_2 (green). The snowflake indicates the absence of emissions due to the freezing of the reservoir surface.

3.4. TOTAL INTEGRATION

Figure 7 shows the total fluxes from the three study areas: the river (upstream and downstream), the study dam, and the control dam. The emissions from the study dam were higher than those from the river before the demolition. However, after the demolition, these total emissions fell within the same range as the river emissions. On the other hand, the emissions from the control dam were quite low, being practically equal to those from the river reaches throughout the entire study period.

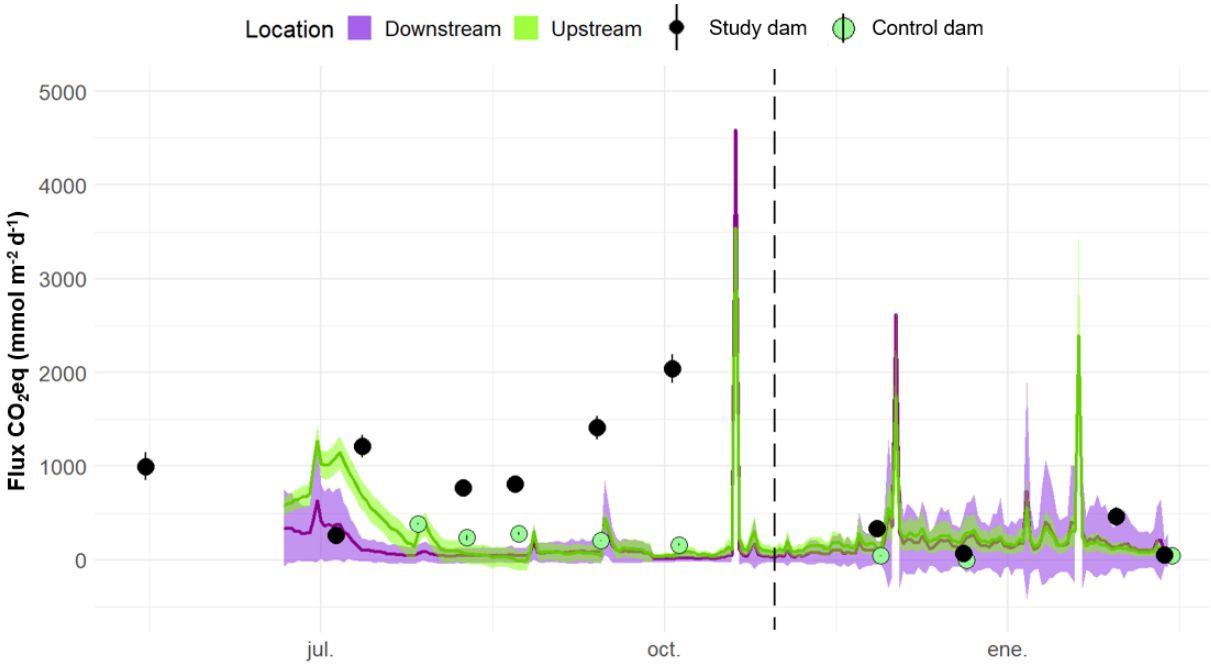

Figure 7: Total fluxes (CO_2, diffusive CH_4, and ebullitive CH_4) expressed in CO_2 equivalents for all study areas: upstream (green solid line) and downstream (purple solid line) river reaches, the study dam (black points), and the control dam (green points), including the associated standard deviations.

4. DISCUSSION

4.1. RIVER EMISSIONS

The total emission values obtained were quite high when compared to other Mediterranean rivers (260 mmol CO_2-eq m^{-2} d^{-1} upstream; 192 mmol CO_2-eq m^{-2} d^{-1} downstream; vs 120 mmol CO_2-eq m^{-2} d^{-1} in the Fluvià and Muga catchment, Gómez-Gener et al., 2015). Usually, high emissions are primarily associated to groundwater inputs of dissolved CO_2 (CH_4 is quite low in streams, <0.3 mmol CO_2-eq m^{-2} d^{-1}; Gómez-Gener et al., 2015) from the decomposition of organic matter in the soil (Jones et al. 2003; Hotchkiss et al. 2015).

However, significant differences have been observed between the total emissions from upstream and downstream sections over the sampling period, although no significant differences were found in their overall averages. This slight difference between the two sections suggests that the presence of the dam can alter the emissions produced downstream, as rivers situated downstream of a dam usually have lower concentrations of GHGs in their waters (Figure 8, Rocher-Ros et al., 2023). However, this difference was minimal, and both river sections followed the same pattern of increase or decrease in emissions. Moreover, this slight difference between the two sections disappeared after the demolition of the dam in mid-November. Consequently, the downstream section seems to have returned to its usual emission levels following the removal of the study dam.

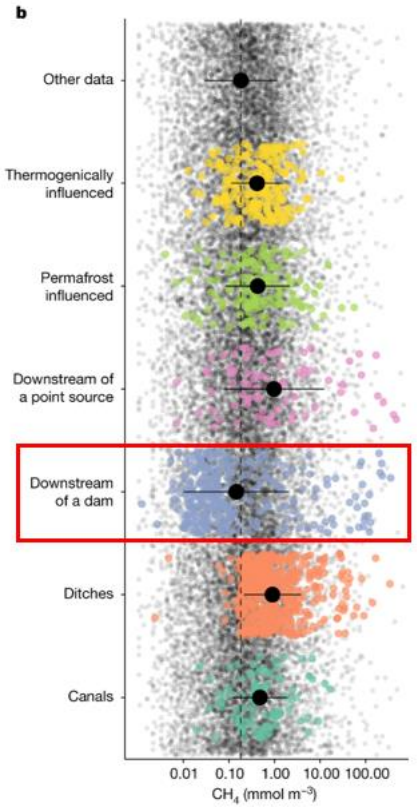

Figure 8: (Main drivers of CH_4 concentrations in streams, Rocher-Ros et al., Nature 2023)

Finally, the presence of large emission peaks corresponded with sudden increases in river flow. This is because the K_{600} (the gas exchange rate) is closely related to the surface turbulence of the water, which is directly linked to changes in the river's geomorphology and hydraulics (Hall & Ulseth, 2019). Thus, a higher flow rate causes greater water speed and turbulence, resulting in higher K_{600} values and, consequently, increased total river emissions. However, since the emission values were estimated from the concentration (interpolated with the values we have) and K_{600} (calculated from water flow values), they could be overestimated. This is because when water flow is higher, the concentrations should be more diluted, resulting in lower values than expected. This factor was not considered in the calculations, and hence, the total emissions during high-flow events may be overestimated.

5.1. REMOVED DAM EMISSIONS

In the studied reservoir, the total GHG emissions decreased after the decommissioning of the dam. On the one hand, there was the seasonal effect. In other studies, the total flux value (CO_2 + CH_4) is positively correlated with the water surface temperature, reaching its maximum value in summer (Xiao et al., 2013). However, while the observed decrease may have some

seasonal influence similar to the control reservoir (see below), the most significant component of the reduction in overall emissions after dam removal in our study dam was the substantial reduction and near disappearance of the CH_4 bubbling emission pathway.

CH_4 production in the sediments depends on several environmental factors, such as water temperature, oxygen concentrations, and nutrient availability (Megonigal et al., 2005). Ebullitive emissions of CH_4 are the dominant pathway in shallow (<50m), stagnant, eutrophic waters where the absence of oxygen upon contact with the sediment leads to anoxic metabolic processes (Bastviken et al., 2011). Moreover, these emissions are quite unpredictable and highly sensitive to changes in water temperature, even more than the diffusive fluxes (Zhang et al., 2020; Zhu et al., 2020). However, with the removal of the dam, the previously stagnant water masses that emitted large amounts of CH_4 are now showing flowing conditions. This renewed movement of water and sediment reduces the likelihood of anoxic conditions, and prevents the accumulation of organic matter on the riverbed, except in a few residual pools. Consequently, this emission pathway almost completely disappeared.

On the other hand, there was an increase in the share of CO_2 emissions respect the total emissions after dam removal (Figure 4), as well as an increase in the absolute value of CO_2 emissions (not shown). After the demolition of the reservoir, much of the area that was previously occupied by water was then sediment exposed directly to the atmosphere. The emissions from this newly exposed sediment were the main source of the increased CO_2 emissions. This sediment was loaded with organic matter, which can be rapidly degraded when it comes into contact with atmospheric oxygen emitting huge amounts of CO_2 (Tesi et al., 2016; Marcé et al., 2019). Previously, this organic matter was not degraded as efficiently due to the lack of oxygen through most of the sediment profile, due to the low solubility of oxygen in water. As this degradation occurs, large amounts of CO_2 are released (Gómez-Gener et al., 2016; Obrador et al., 2018).

In the study reservoir, ebullitive CH_4 emissions were responsible for a large share of total emissions before dam removal. Therefore, their reduction has compensated for the moderate increase in CO_2 from the sediment. Thus, although new fluxes from the exposed sediment appeared, the overall C emissions were lower than those present before the dam was demolished. However, it is important to emphasize that this is not always the case for all dams. If the emissions prior to demolition are relatively low and there is not much CH_4 bubbling, it is possible that after demolition, the fluxes may increase due to the degradation of organic matter from the exposed accumulated sediment and subsequent increased CO_2 emissions (Amani et al., 2022).

One important limitation of this study was the lack of data for at least one entire year before and after the demolition. Thus, it is possible that total emissions after removal could increase with the arrival of warmer weather in summer, especially from the exposed sediments, as higher temperatures can accelerate the degradation of organic matter (Keller et al., 2021). However, we do not expect this to occur in our study site. On one hand, the fluxes from the now flowing water within the previous dam should now follow the same pattern as those in the upstream and downstream sections of the river, which did maintain the same average total emission value throughout the entire period. Therefore, we expect that with the dam removal, a similar pattern will emerge in the newly created river section. On the other hand, there are emissions from the sediment. In this case, bare and exposed sediment may increase its emissions as the temperature rises (Keller et al., 2021). However, this phenomenon is not expected in the context of our study reservoir. The sediment has been and continues to be colonized by extensive native vegetation, which through primary succession has almost completely covered the previously exposed sediment. This vegetation cover changes the total net emissions from the exposed sediment. It has been observed that in reservoirs that have dried up or been removed, sediment emissions decrease once they are colonized by vegetation, even showing negative net fluxes (Amani et al., 2022; Sharma et al., publication in process). Therefore, due to this rapid succession, we do not expect sediment emissions to increase with the change in seasons. Overall, the total emissions from this reservoir have decreased following its demolition, and we do not expect them to increase again over time.

5.2. CONTROL DAM EMISSIONS

The control reservoir was characterized by having lower emissions compared to the study reservoir. These emissions decreased seasonally with the arrival of winter and colder temperatures, with a progressive and stepped decline throughout the sampling period, reaching a minimum in December when the reservoir completely froze. Therefore, we expect the observed pattern to be cyclical, with total emissions increasing again in the spring. Conversely, while it is plausible that the study dam also experienced a seasonal effect causing a decrease in total emissions, the pattern was neither as clear nor as stepped, making it difficult to attribute the total observed decrease solely to seasonality.

Additionally, this reservoir almost entirely lacked the CH_4 bubbling emission pathway. In most incubations conducted, it was not even detectable, resulting in much lower values than those of the study reservoir. This type of emission is quite unpredictable, although it typically follows a seasonal decrease between summer and winter (de Mello et al., 2017), not observed in the control dam.

This difference between the two reservoirs may be due to the control reservoir having less riparian forest around it and being more open, leading to greater solar incidence and a reduced input of allochthonous organic matter into the system. Reduced input of organic matter causes the waters to be more oligotrophic than in the studied reservoir, a fact that is visibly noticeable as its water is clearer, and the bottom of the reservoir was often covered with green filamentous algae. Thus, it is a less productive system, leading to less organic matter accumulating at the bottom and a more oxygenated water. Given these characteristics, the generation of CH_4 bubbles is more difficult (DelSontro et al., 2016). Therefore, the absence of this emission pathway is primarily responsible for the differences observed between the two reservoirs.

As a result, although the control reservoir is in the same watershed, just a few kilometres from the study reservoir, it has proven to be an unsuitable control due to its feeble CH_4 bubbling emissions. However, the fact that this reservoir shows a clear seasonal pattern must be considered when interpreting the data obtained in the removed dam.

5.3. TOTAL INTEGRATION

Overall, our results show that anthropogenic greenhouse gas (GHG) emissions from a Mediterranean reservoir, especially CH_4, decrease when the dam is dismantled and river continuity is restored. As we expected, before the removal of the dam, the total GHG emissions were lower in the free-flowing river sections compared to the dammed sections. Moreover, significant differences were found over time between the two river sections studied, upstream and downstream from the dam. Therefore, the interruption of the river flow by the dam causes an increase in GHG emissions to the atmosphere. Additionally, it alters the downstream river biogeochemistry, which differs from the undisturbed upstream section.

This phenomenon has been observed in multiple reservoirs worldwide (Downing et al., 2008), as the slowed water flow allows for greater accumulation of nutrients and organic matter, which are more extensively decomposed in the reservoir waters, and specially, sediments (DelSontro et al. 2016). While the implications of CO_2 emissions from reservoirs on the anthropogenic GHG inventories are ambiguous, as they can sometimes capture CO_2 instead of emitting it, CH_4 emissions are highly detrimental and, in our case, very abundant and of clear anthropogenic origin.

On the other hand, emissions change completely after the demolition of the dam. Firstly, we have the total emissions from the two river reaches. After the dam was demolished, there were no longer significant differences between the two river reaches. Thus, the downstream section of the river is no longer biogeochemically disturbed by the presence of the dam, and it recovers

its original emission values (equal to upstream). Furthermore, as we hypothesized, the total emissions from the study reservoir decreased after the demolition. Consequently, an anthropogenic hotspot of emission, primarily CH_4, has been removed.

Based on the results of our study, we can assert that the removal of unused dams can be an effective method for reducing and mitigating anthropogenic GHG emissions. Thus, dam removal offers broad ecological and environmental benefits. It not only reduces GHG emissions but also restores natural river flow and enhances habitat connectivity, leading to increased biodiversity and healthier ecosystems. Additionally, it provides social and economic benefits, reducing the maintenance costs. Overall, our study highlights the importance of dam removal as a comprehensive strategy for environmental restoration and climate change mitigation.

5. CONCLUSION

The main result of this study was that anthropogenic greenhouse gas (GHG) emissions from a dammed stretch of a Mediterranean river network decreased when the dam was dismantled and flow continuity was restored. We conclude that:

- There was negligible annual variability in GHG emissions from the upstream and downstream riverine sites. However, differences existed between the two sites before the dam's removal. These differences disappeared after the removal, indicating that the downstream site had been perturbed before the removal and was restored afterward.
- Before the removal, total emissions were higher in the reservoir compared to the river sites. After the removal, emissions in both locations fell within the same range.
- Total emissions from the studied reservoir decreased, even when accounting for the new emissions from the exposed sediment.
- There was seasonal variability in the total emissions from dams, particularly noticeable in the control reservoir.
- Dam removal demonstrated potential to reduce anthropogenic GHG emissions, thereby contributing to the decarbonization of the hydrological landscape.

6. BIBLIOGRAPHY

Amani, M., von Schiller, D., Suárez, I., Atristain, M., Elosegi, A., Marcé, R., García-Baquero, G., & Obrador, B. (2022). The drawdown phase of dam decommissioning is a hot moment of gaseous carbon emissions from a temperate reservoir. Inland Waters, 12(4), 451–462. https://doi.org/10.1080/20442041.2022.2096977

Aufdenkampe, A. K., Mayorga, E., Raymond, P. A., Melack, J. M., Doney, S. C., Alin, S. R., Aalto, R. E., & Yoo, K. (2011). Riverine coupling of biogeochemical cycles between land, oceans, and atmosphere. Frontiers in Ecology and the Environment, 9(1), 53–60. https://doi.org/10.1890/100014

Bastviken, D., Cole, J., Pace, M., & Tranvik, L. (2004). Methane emissions from lakes: Dependence on lake characteristics, two regional assessments, and a global estimate. Global Biogeochemical Cycles, 18(4), 1–12. https://doi.org/10.1029/2004GB002238

Bastviken, D., Cole, J. J., Pace, M. L., & van de-Bogert, M. C. (2008). Fates of methane from different lake habitats: Connecting whole-lake budgets and CH4 emissions. Journal of Geophysical Research: Biogeosciences, 113(2). https://doi.org/10.1029/2007JG000608

Bastviken, D., Tranvik, L. J., Downing, J. A., Crill, P. M., & Enrich-Prast, A. (2011). Freshwater methane emissions offset the continental carbon sink. Science, 331(6013), 50. https://doi.org/10.1126/science.1196808

Battin, T. J., Luyssaert, S., Kaplan, L. A., Aufdenkampe, A. K., Richter, A., & Tranvik, L. J. (2009). The boundless carbon cycle. Nature Geoscience, 2(10), 598–600. https://doi.org/10.1038/ngeo618

Borges, A. V., Darchambeau, F., Teodoru, C. R., Marwick, T. R., Tamooh, F., Geeraert, N., Omengo, F. O., Guérin, F., Lambert, T., Morana, C., Okuku, E., & Bouillon, S. (2015). Globally significant greenhouse-gas emissions from African inland waters. Nature Geoscience, 8(7), 637–642. https://doi.org/10.1038/ngeo2486

Cole, J. J., Prairie, Y. T., Caraco, N. F., McDowell, W. H., Tranvik, L. J., Striegl, R. G., Duarte, C. M., Kortelainen, P., Downing, J. A., Middelburg, J., & Melack, J. (2007). Plumbing the global carbon cycle: Integrating inland waters into the terrestrial carbon budget. Ecosystems, 10(2), 171–184. https://doi.org/10.1007/s10021-006-9013-8

Deemer, B. R., Harrison, J. A., Li, S., Beaulieu, J. J., DelSontro, T., Barros, N., Bezerra-Neto, J. F., Powers, S. M., dos Santos, M. A., & Vonk, J. A. (2016). Greenhouse gas emissions from reservoir water surfaces: A new global synthesis. Bioscience, 66(11), 949–964. https://doi.org/10.1093/biosci/biw117

DelSontro, T., Boutet, L., St-Pierre, A., del Giorgio, P. A., & Prairie, Y. T. (2016). Methane ebullition and diffusion from northern ponds and lakes regulated by the interaction between temperature and system productivity. Limnology and Oceanography, 61(S1), S62–S77. https://doi.org/10.1002/lno.10335

de Mello, N. A. S. T., Brighenti, L. S., Barbosa, F. A. R., Staehr, P. A., & Bezerra Neto, J. F. (2017). Spatial variability of methane (CH4) ebullition in a tropical hypereutrophic reservoir: Silted areas as a bubble hot spot. Lake and Reservoir Management, 34(2), 105–114. https://doi.org/10.1080/10402381.2017.1390018

Doyle, M. W., Stanley, E. H., Harbor, J. M., & Grant, G. S. (2003). Dam removal in the United States: Emerging needs for science and policy. Eos, 84(4), 36–40. https://doi.org/10.1029/2003EO040001

Donohue, I., & Molinos, J. G. (2009). Impacts of increased sediment loads on the ecology of lakes. Biological Reviews, 84(4), 517–531. https://doi.org/10.1111/j.1469-185X.2009.00081.x

Downing, J. A., Cole, J. J., Middelburg, J. J., Striegl, R. G., Duarte, C. M., Kortelainen, P., Prairie, Y. T., & Laube, K. A. (2008). Sediment organic carbon burial in agriculturally eutrophic impoundments over the last century. Global Biogeochemical Cycles, 22(4), GB1028. https://doi.org/10.1029/2007GB002963

Duc, N. T., Crill, P., & Bastviken, D. (2010). Implications of temperature and sediment characteristics on methane formation and oxidation in lake sediments. Biogeochemistry, 100(2), 185–196. https://doi.org/10.1007/s10533-010-9415-8

Dudgeon, D., Arthington, A. H., Gessner, M. O., Kawabata, Z. I., Knowler, D. J., Leveque, C., Naiman, R. J., Prieur-Richard, A. H., Soto, D., Stiassny, M. L. J., & Sullivan, C. A. (2006). Freshwater biodiversity: Importance, threats, status and conservation challenges. Biological Reviews, 81(2), 163–182. https://doi.org/10.1017/S1464793105006950

Engle, D., & Melack, J. M. (2000). Methane emissions from an Amazon floodplain lake: Enhanced release during episodic mixing and during falling water. Biogeochemistry, 51(1), 71–90. https://doi.org/10.1023/A:1006389124823

Eugster, W., DelSontro, T., & Sobek, S. (2011). Eddy covariance flux measurements confirm extreme CH4 emissions from a Swiss hydropower reservoir and resolve their short-term variability. Biogeosciences, 8(9), 2815–2831. https://doi.org/10.5194/bg-8-2815-2011

Fang, J., Wang, Z., Zhao, S., Li, Y., Tang, Z., Yu, D., Ni, L., Liu, H., Xie, P., Da, L., Li, Z., & Zheng, C. (2006). Biodiversity changes in the lakes of the central Yangtze. Frontiers in Ecology and the Environment, 4(7), 369–377. https://doi.org/10.1890/1540-9295(2006)4[369:BCITLO]2.0.CO;2

Farrelly, D. J., Everard, C. D., Fagan, C. C., & McDonnell, K. P. (2013). Carbon sequestration and the role of biological carbon mitigation: A review. Renewable and Sustainable Energy Reviews, Elsevier Ltd. 21, 712–727. https://doi.org/10.1016/j.rser.2012.12.038

Friedlingstein, P., O'Sullivan, M., Jones, M. W., Andrew, R. M., Hauck, J., Olsen, A., Peters, G. P., Peters, W., … & Zaehle, S. (2020). Global carbon budget 2020. Earth System Science Data, 12, 3269–3340. https://doi.org/10.5194/essd-12-3269-2020

Gómez-Gener, L., Obrador, B., von Schiller, D., Marcé, R., Casas-Ruiz, J. P., & Proia, L. (2015). Hot spots for carbon emissions from Mediterranean fluvial networks during summer drought. Biogeochemistry, 125(3), 409–426. https://doi.org/10.1007/s10533-015-0128-7

Gómez-Gener, L., Obrador, B., Marcé, R., Acuña, V., Catalán, N., Casas-Ruiz, J. P., & Sabater, S. (2016). When water vanishes: Magnitude and regulation of carbon dioxide

emissions from dry temporary streams. Ecosystems, 19(4), 710–723. https://doi.org/10.1007/s10021-016-9963-4

Gómez-Gener, L., Gubau, M., von Schiller, D., Marcé, R., & Obrador, B. (2023). Integrated assessment of the net carbon footprint of small hydropower plants. *Environmental Research Letters*, *18*(8). https://doi.org/10.1088/1748-9326/acdfe5

Hall, R. O., Jr., & Ulseth, A. J. (2019). Gas exchange in streams and rivers. WIREs Water, 7(1), e1391. https://doi.org/10.1002/wat2.1391

Hotchkiss, E. R., Hall, R. O., Sponseller, R. A., Butman, D., Klaminder, J., Laudon, H., & Rosvall, M. (2015). Sources of and processes controlling CO2 emissions change with the size of streams and rivers. Nature Geoscience, 8(8), 696–699. https://doi.org/10.1038/ngeo2507

[IPCC] Intergovernmental Panel on Climate Change. (2021). Climate change 2021: The physical science basis (Contribution of Working Group I to the Sixth Assessment Report of the Intergovernmental Panel on Climate Change). Cambridge University Press. https://www.ipcc.ch/report/ar6/wg1/

[IPCC] Intergovernmental Panel on Climate Change. (2019). 2019 Refinement to the 2006 IPCC guidelines for national greenhouse gas inventories, Volume 4. Retrieved December 24, 2019, from https://www.ipcc-nggip.iges.or.jp/public/2019rf/index.html

Jin, H. S., White, D. S., Ramsey, J. B., & Kipphut, G. W. (2012). Mixed tracer injection method to measure reaeration coefficients in small streams. Water, Air, & Soil Pollution, 223(8), 5297–5306. https://doi.org/10.1007/s11270-012-1296-6

Johnson, M. S., Matthews, E., Bastviken, D., Deemer, B., Du, J., & Genovese, V. (2021). Spatiotemporal methane emission from global reservoirs. Journal of Geophysical Research: Biogeosciences, 126(8). https://doi.org/10.1029/2021JG006305

Jones, J. B., Stanley, E. H., & Mulholland, P. J. (2003). Long-term decline in carbon dioxide supersaturation in rivers across the contiguous United States. Geophysical Research Letters, 30(4), 1495. https://doi.org/10.1029/2003GL017056

Keller, M., & Stallard, R. F. (1994). Methane emission by bubbling from Gatun Lake, Panama. Journal of Geophysical Research: Atmospheres, 99(D5), 8307–8319. https://doi.org/10.1029/92JD02170

Keller, P. S., Catalán, N., von Schiller, D., Grossart, H. P., Koschorreck, M., Obrador, B., Frassl, M. A., Karakaya, N., Barros, N., Howitt, J. A., et al. (2020). Global CO2 emissions from dry inland waters share common drivers across ecosystems. Nature Communications, 11, 1–8. https://doi.org/10.1038/s41467-020-15929-y

Keller, P. S., Marcé, R., Obrador, B., & Koschorreck, M. (2021). Global carbon budget of reservoirs is overturned by the quantification of drawdown areas. Nature Geoscience, 14, 402–408. https://doi.org/10.1038/s41561-021-00737-w

Kirchherr, J., & Charles, K. J. (2016). The social impacts of dams: A new framework for scholarly analysis. Environmental Impact Assessment Review, 60, 99–114. https://doi.org/10.1016/j.eiar.2016.02.005

Kirschke, S., Bousquet, P., Ciais, P., Saunois, M., Canadell, J. G., Dlugokencky, E. J., Bergamaschi, P., Bergmann, D., Blake, D. R., … & Zeng, G. (2013). Three decades of

global methane sources and sinks. Nature Geoscience, 6, 813–823. https://doi.org/10.1038/ngeo1955

Lal, R. (2007). Carbon sequestration. Philosophical Transactions of the Royal Society B: Biological Sciences. https://doi.org/10.1098/rstb.2007.2185

Lehner, B., Liermann, C. R., Revenga, C., Vörösmarty, C., Fekete, B., Crouzet, P., Döll, P., Endejan, M., Frenken, K., Magome, J., Nilsson, C., Robertson, J., Rödel, R., Sindorf, N., & Wisser, D. (2011). High-resolution mapping of the world's reservoirs and dams for sustainable river-flow management. Frontiers in Ecology and the Environment, 9(9), 494–502. https://doi.org/10.1890/100125

Maavara, T., Chen, Q., Van Meter, K., Brown, L. E., Zhang, J., Ni, J., & Zarfl, C. (2020). River dam impacts on biogeochemical cycling. Nature Reviews Earth & Environment, 1(2), 103–116. https://doi.org/10.1038/s43017-019-0019-0

Marcé, R., Obrador, B., Gómez-Gener, L., Catalán, N., Koschorreck, M., Arce, M. I., Singer, G., & von Schiller, D. (2019). Emissions from dry inland waters are a blind spot in the global carbon cycle. In Earth-Science Reviews (Vol. 188, pp. 240–248). Elsevier B.V. https://doi.org/10.1016/j.earscirev.2018.11.012

Megonigal, J. P., Mines, M. E., & Visscher, P. T. (2005). Linkages to trace gases and aerobic processes. Biogeochemistry, 8, 350–362.

Mendonça, R., Müller, R. A., Clow, D., Verpoorter, C., Raymond, P., Tranvik, L., & Sobek, S. (2017). Organic carbon burial in global lakes and reservoirs. Nature Communications, 8, 1694. https://doi.org/10.1038/s41467-017-01796-4

Obrador, B., von Schiller, D., Marcé, R., Gómez-Gener, L., Koschorreck, M., Borrego, C., & Catalán, N. (2018). Dry habitats sustain high CO2 emissions from temporary ponds across seasons. Scientific Reports, 8, 3015. https://doi.org/10.1038/s41598-018-21357-y

Perera, D., & North, T. (2021). The socio-economic impacts of aged-dam removal: A review. Journal of Geoscience and Environment Protection, 9(10), 81–95. https://doi.org/10.4236/gep.2021.910005

Raymond, P. A., Zappa, C. J., Butman, D., Bott, T. L., Potter, J., Mulholland, P., … & Newbold, D. (2012). Scaling the gas transfer velocity and hydraulic geometry in streams and small rivers. Limnology and Oceanography: Fluids and Environments, 2(1), 41–53. https://doi.org/10.1215/21573689-1583715

Raymond, P., Hartmann, J., Lauerwald, R., … & Cole, J. J. (2013). Global carbon dioxide emissions from inland waters. Nature, 503(7476), 355–359. https://doi.org/10.1038/nature12760

Rocher-Ros, G., Stanley, E. H., Loken, L. C., Casson, N. J., Raymond, P. A., Liu, S., Amatulli, G., & Sponseller, R. A. (2023). Global methane emissions from rivers and streams. Nature, 621(7979), 530–535. https://doi.org/10.1038/s41586-023-06344-6

Schiermeier, Q. (2018). Europe is demolishing its dams to restore ecosystems. Nature, 557, 290–291. https://doi.org/10.1038/d41586-018-05182-1

Spiess, A.-N. (2018). propagate: Propagation of Uncertainty (Version 1.0-6) [R package]. CRAN. https://CRAN.R-project.org/package=propagate

Stanley, E. H., Casson, N. J., Crawford, J. T., Loken, L. C., & Oliver, S. K. (2016). The ecology of methane in streams and rivers: Patterns, controls, and global significance. Ecological Monographs, 86(2), 146–171. https://doi.org/10.1890/15-1027

Tesi, T., Muschitiello, F., Smittenberg, R. H., Jakobsson, M., Vonk, J. E., Hill, P., Andersson, A., Kirchner, N., Noormets, R., Dudarev, O., Semiletov, I., & Gustafsson. (2016). Massive remobilization of permafrost carbon during post-glacial warming. Nature Communications, 7. https://doi.org/10.1038/ncomms13653

Vorosmarty, C. J., McIntyre, P. B., Gessner, M. O., Dudgeon, D., Prusevich, A., Green, P., Glidden, S., Bunn, S. E., Sullivan, C. A., & et al. (2010). Global threats to human water security and river biodiversity. Nature, 467, 555–561. https://doi.org/10.1038/nature09440

Wu, H., Zeng, G., Liang, J., Zhang, J., Cai, Q., Huang, L., Li, X., Zhu, H., Hu, C., & et al. (2013). Changes of soil microbial biomass and bacterial community structure in Dongting Lake: Impacts of 50,000 dams of Yangtze River. Ecological Engineering, 57, 72–78. https://doi.org/10.1016/j.ecoleng.2013.04.038

Wu, H., Chen, J., Xu, J., Zeng, G., Sang, L., Liu, Q., Yin, Z., Dai, J., Yin, D., & et al. (2019). Effects of dam construction on biodiversity: A review. Journal of Cleaner Production, 221, 480–489. https://doi.org/10.1016/j.jclepro.2019.03.001

Xiao, S., Wang, Y., Liu, D., Yang, Z., Lei, D., & et al. (2013). Diel and seasonal variation of methane and carbon dioxide fluxes at Site Guojiaba, the Three Gorges Reservoir. Journal of Environmental Sciences (China), 25(10), 2065–2071. https://doi.org/10.1016/S1001-0742(12)60269-1

Yamamoto, S., Alcauskas, J. B., Crozier, T. E., & et al. (1976). Solubility of methane in distilled water and seawater. Journal of Chemical & Engineering Data, 21, 78–80. https://doi.org/10.1021/je60068a029

Yang, M., Geng, X., Grace, J., Lu, C., Zhu, Y., Zhou, Y., & et al. (2014). Spatial and seasonal CH4 flux in the littoral zone of Miyun Reservoir near Beijing: The effects of water level and fluctuation. PLoS ONE, 9(4), e94275. https://doi.org/10.1371/journal.pone.0094275

Zhang, W., Xiao, S., Xie, H., Liu, J., Lei, D., Lorke, A., & et al. (2020). Diel and seasonal variability of methane emissions from a shallow and eutrophic pond. Biogeosciences Discussions, 1–40. https://doi.org/10.5194/bg-2020-178

Zhu, Y., Purdy, K. J., Eyice, Ö., Shen, L., Harpenslager, S. F., Yvon-Durocher, G., & et al. (2020). Disproportionate increase in freshwater methane emissions induced by experimental warming. Nature Climate Change, 10, 685–690. https://doi.org/10.1038/s41558-020-0824-y